

A New-Generation Internal Tide Model Based on 30 Years of Satellite Sea Surface Height Measurements

Zhongxiang Zhao ^{1,2}

¹ *Applied Physics Laboratory, University of Washington, Seattle, Washington, USA*

² *School of Oceanography, University of Washington, Seattle, Washington, USA*

Corresponding author: Zhongxiang Zhao, zzhao@uw.edu

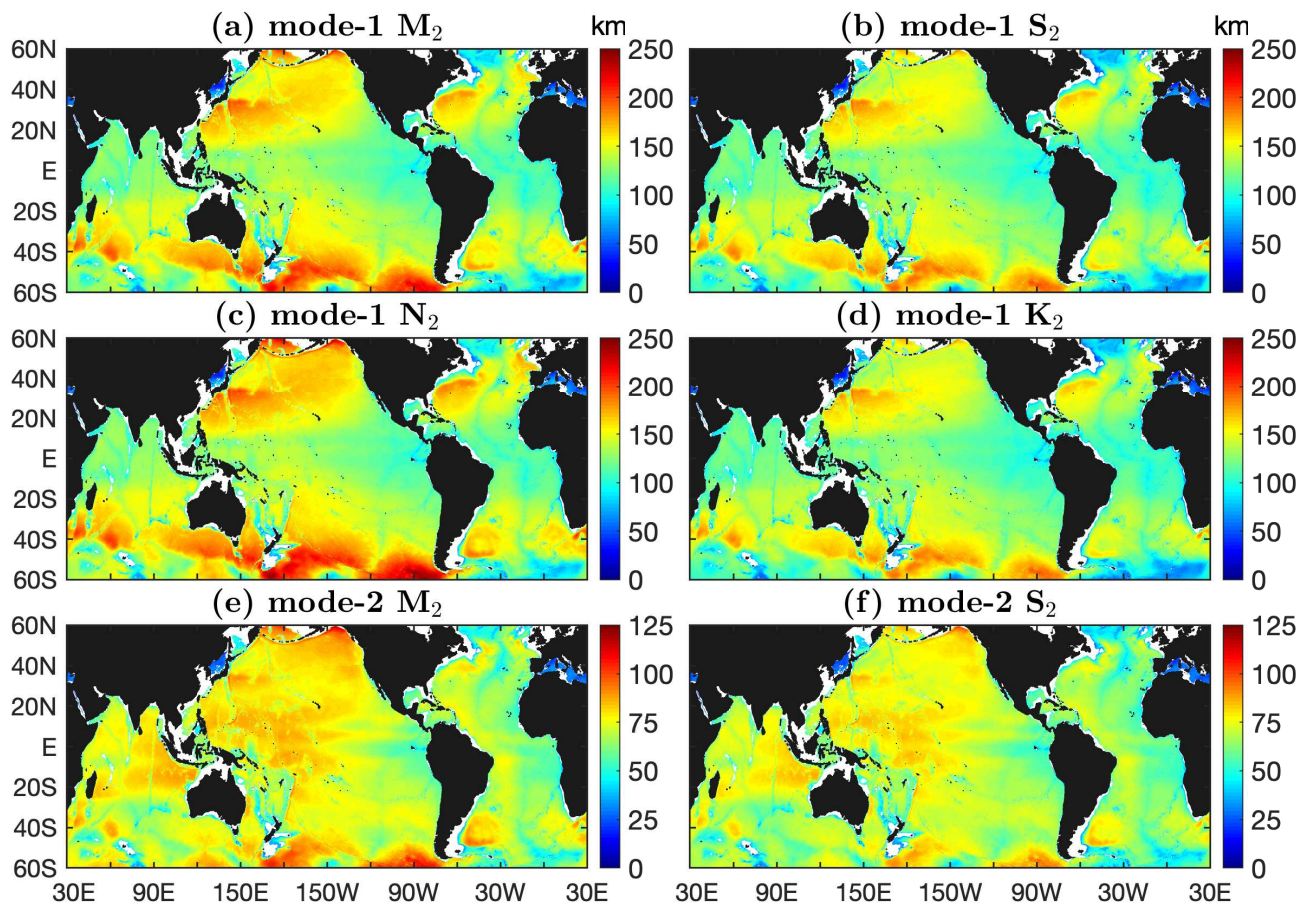


Figure S1. Wavelengths of semidiurnal internal tides obtained by solving the Sturm-Liouville orthogonal problem using the climatological annual-mean hydrographic profiles in the World Ocean Atlas 2018 and the dispersion relation of linear internal gravity waves with Earth's rotation.

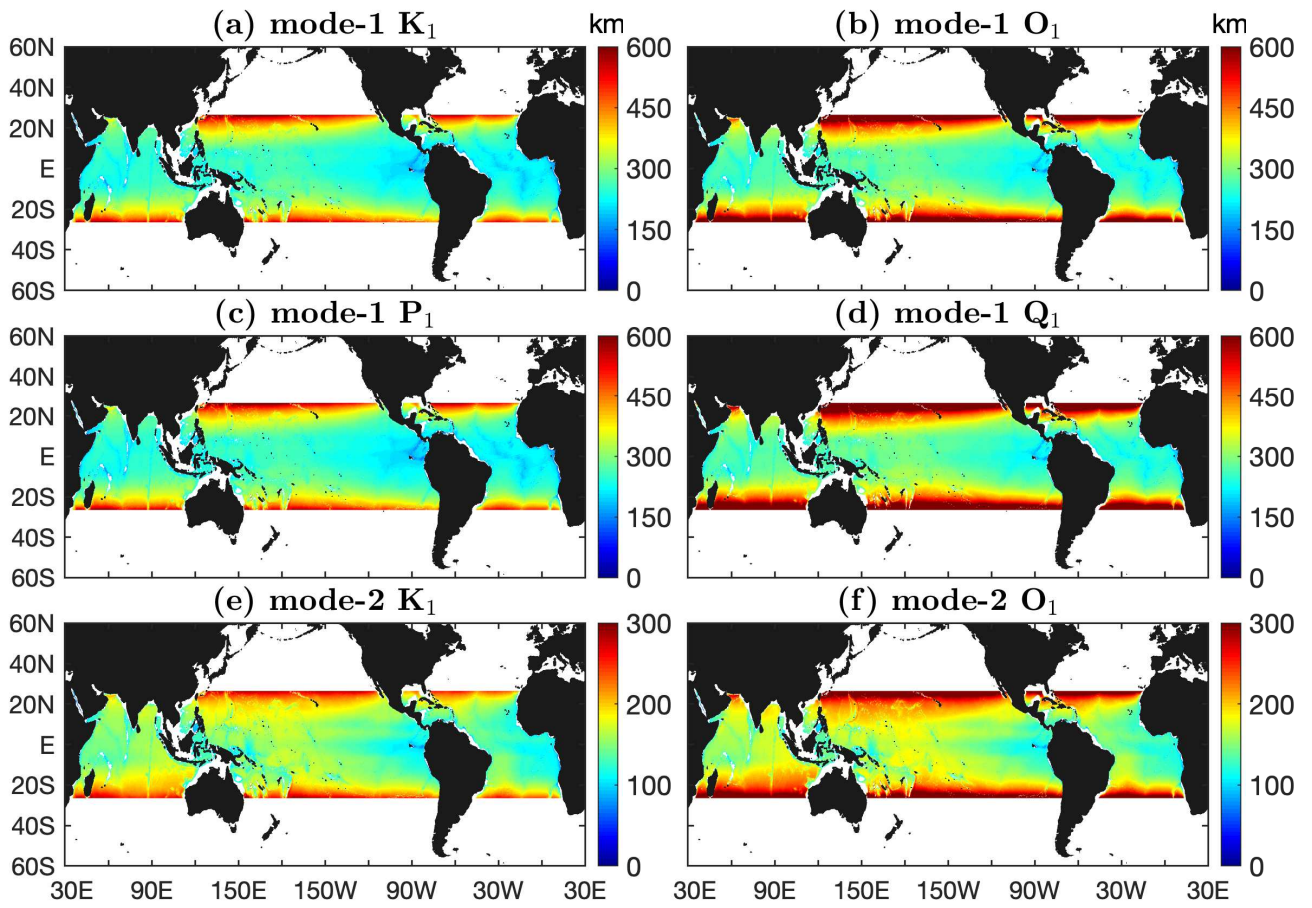


Figure S2. As in Figure S1 but for diurnal internal tides.

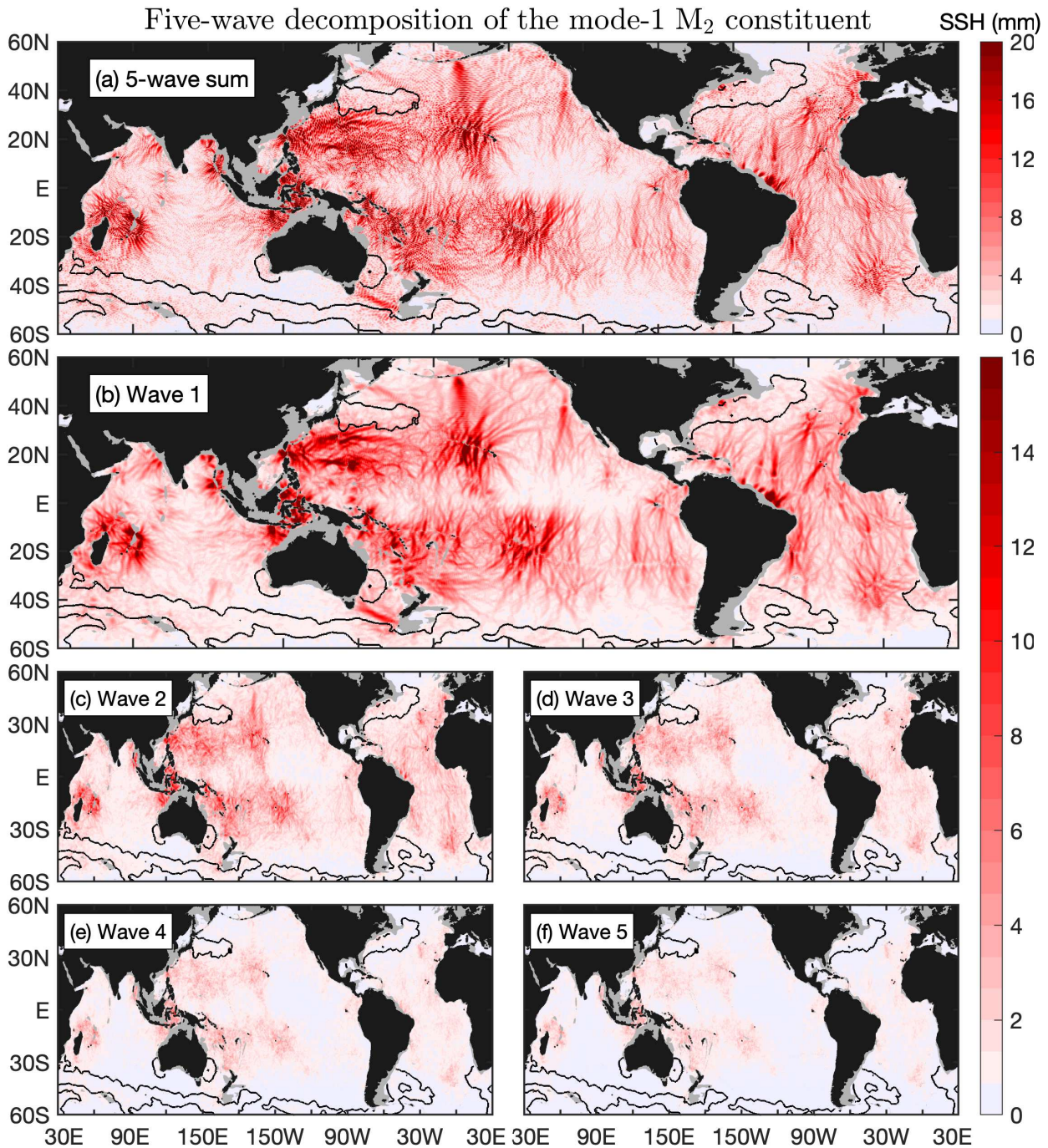


Figure S3. Five-wave decomposition of the mode-1 M_2 internal tide constituent. (a) The 5-wave sum. (b)-(f) The 5 waves. At each grid point, five mode-1 M_2 internal tidal waves in arbitrary horizontal directions are determined by plane wave analysis. Black contours indicate regions of large model errors. Panel (b) shows well-defined long-range internal tidal beams associated with notable topographic features.

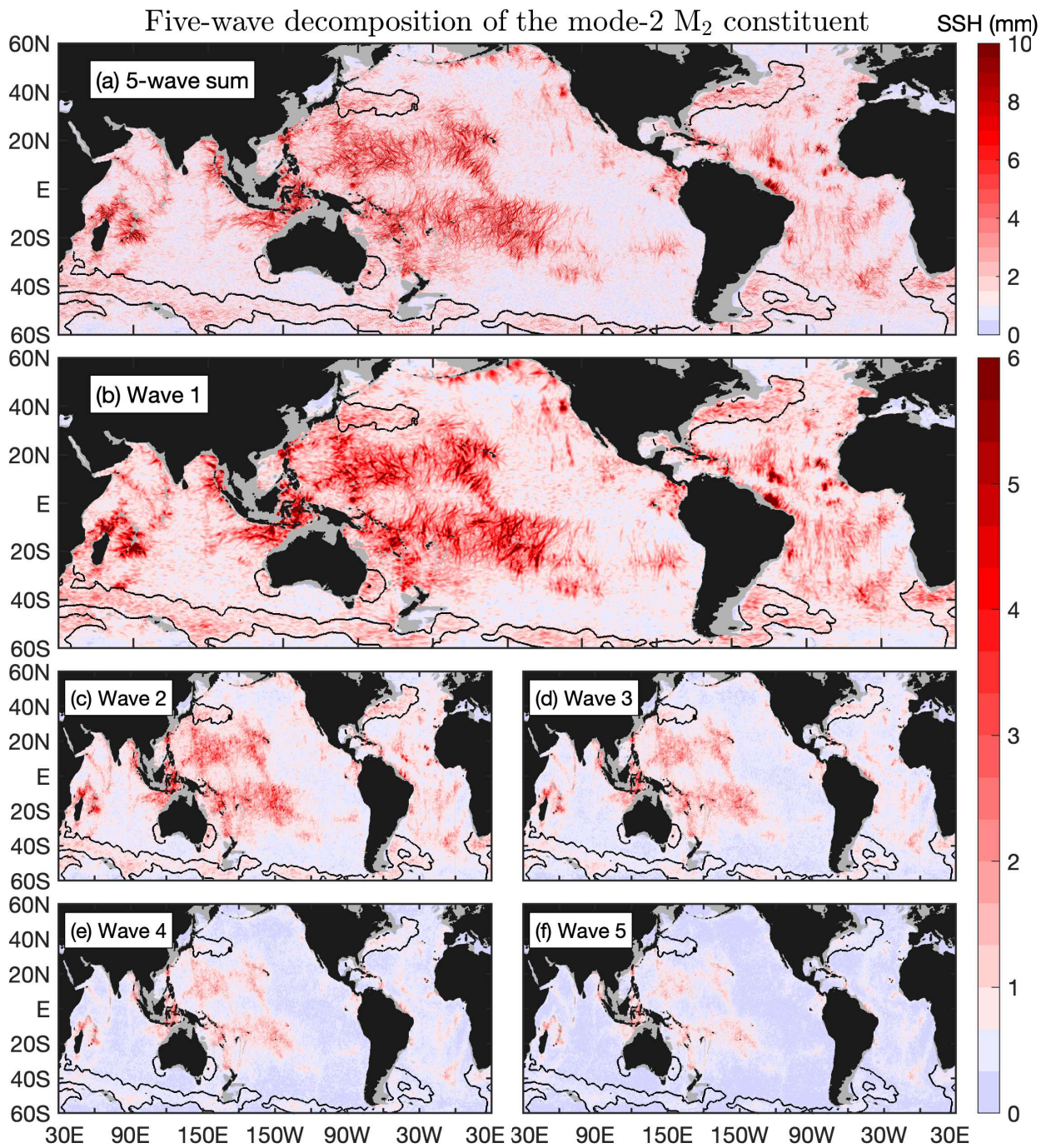


Figure S4. As in Figure S3 but for the mode-2 M_2 internal tide constituent.

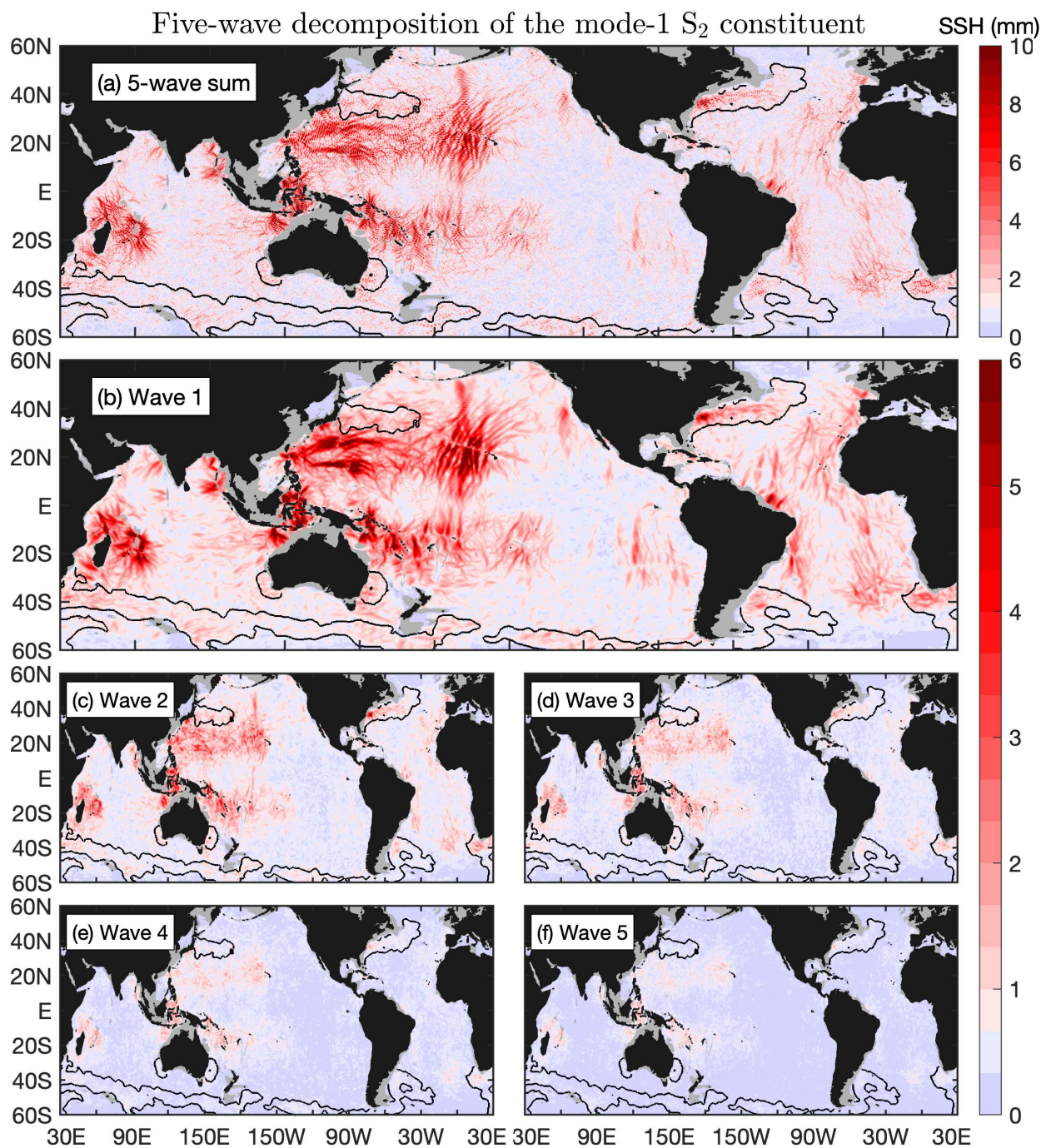


Figure S5. As in Figure S3 but for the mode-1 S_2 internal tide constituent.

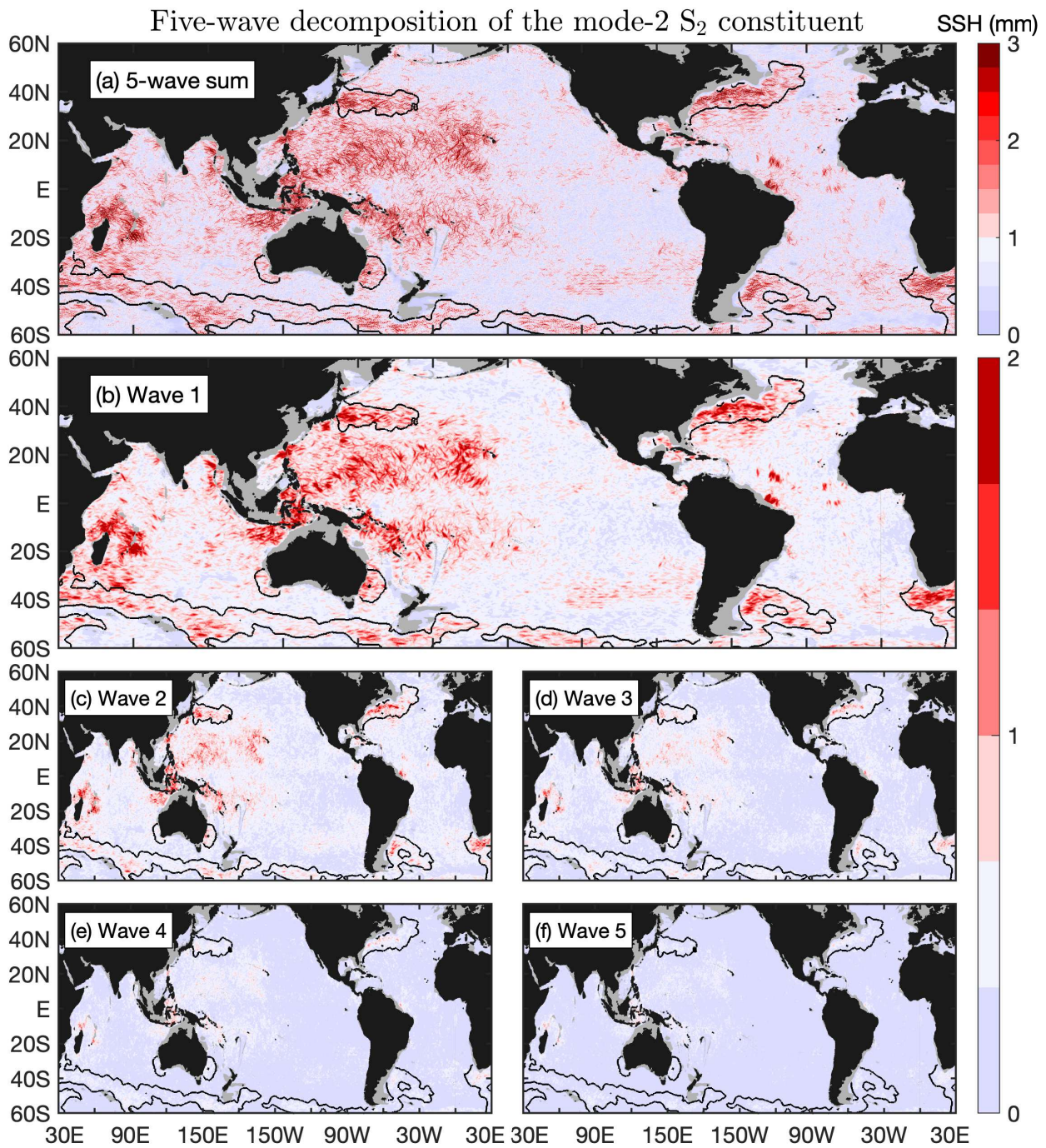


Figure S6. As in Figure S4 but for the mode-2 S_2 internal tide constituent.

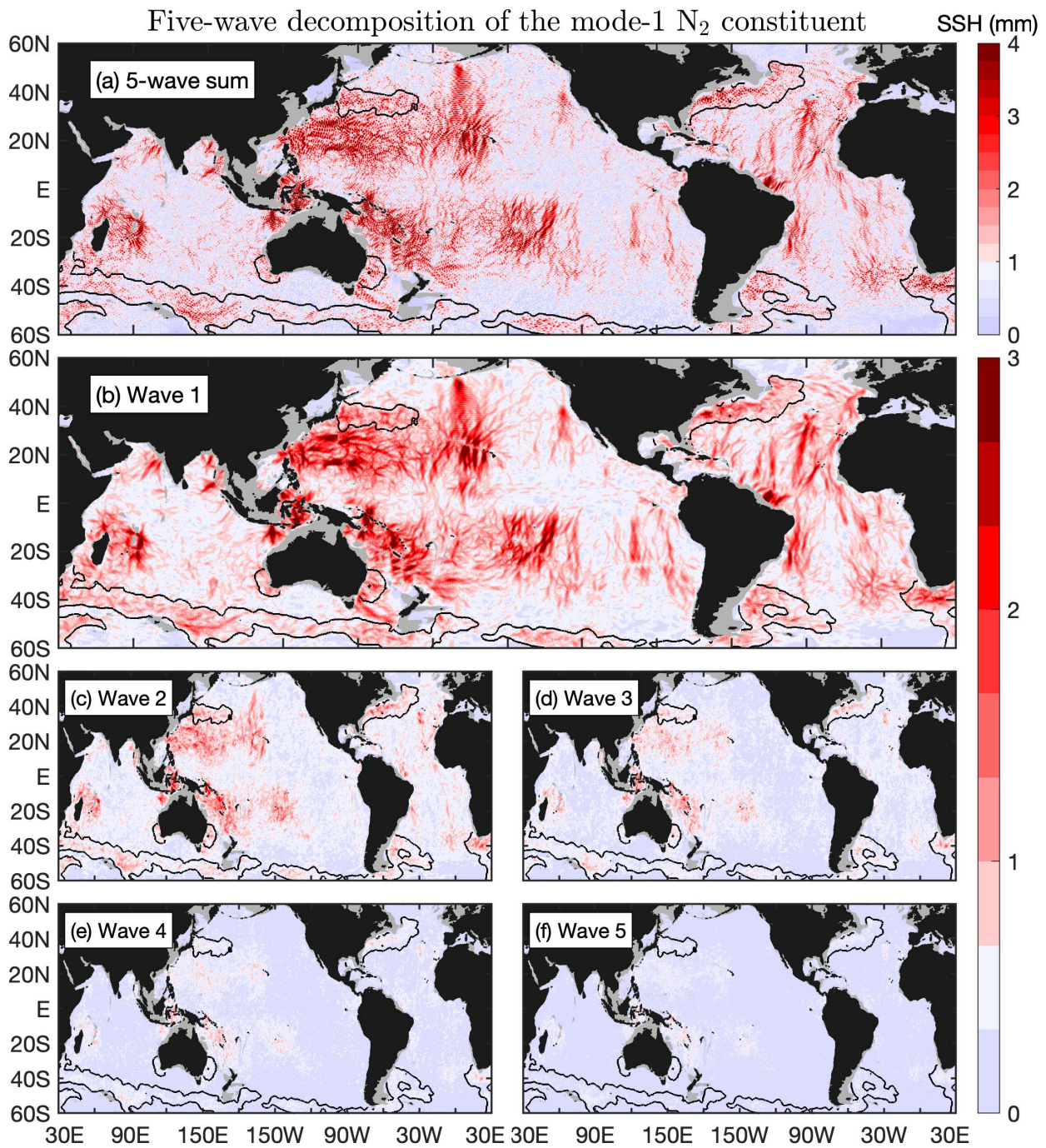


Figure S7. As in Figure S3 but for the mode-1 N_2 internal tide constituent.

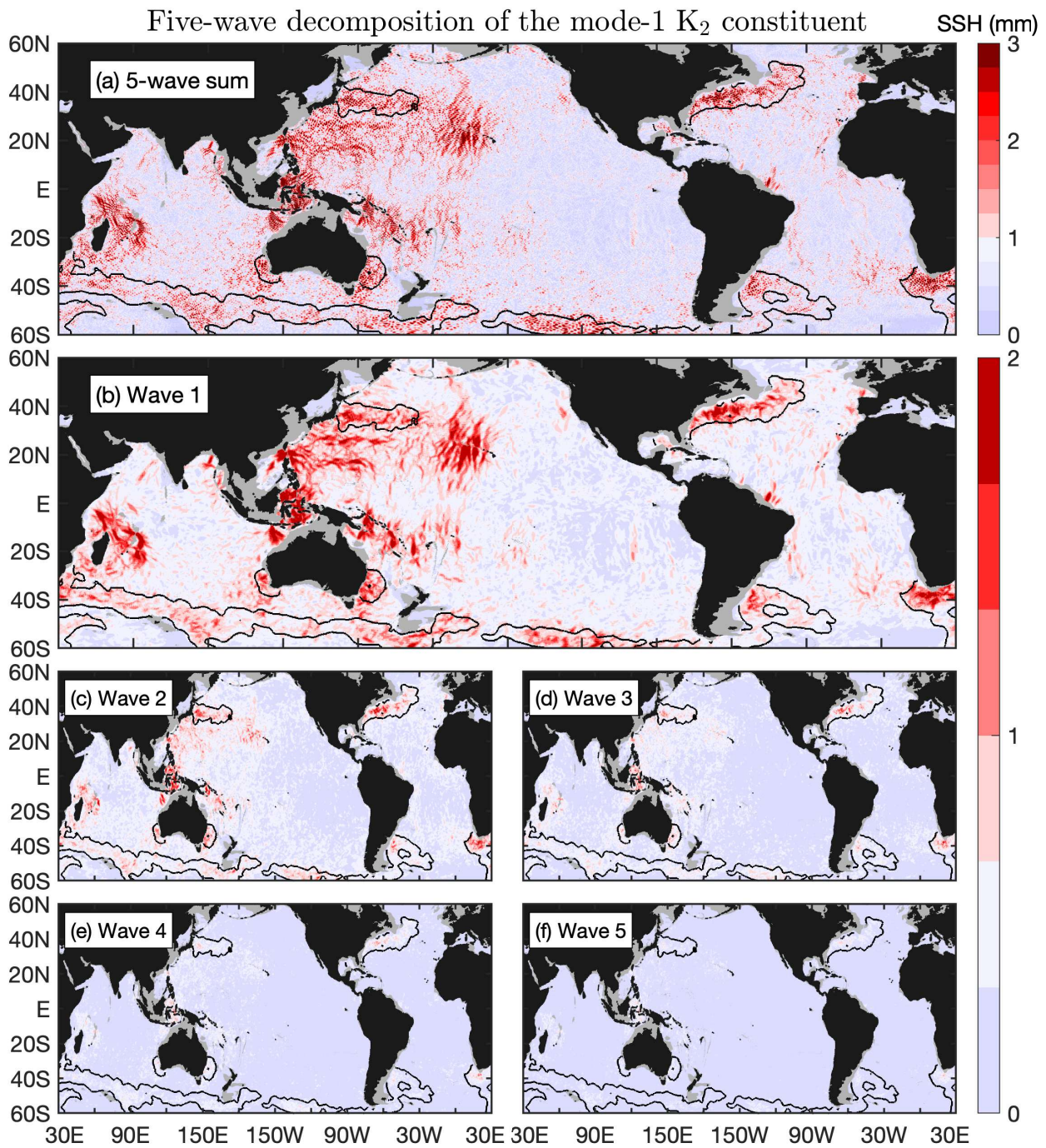


Figure S8. As in Figure S3 but for the mode-1 K_2 internal tide constituent.

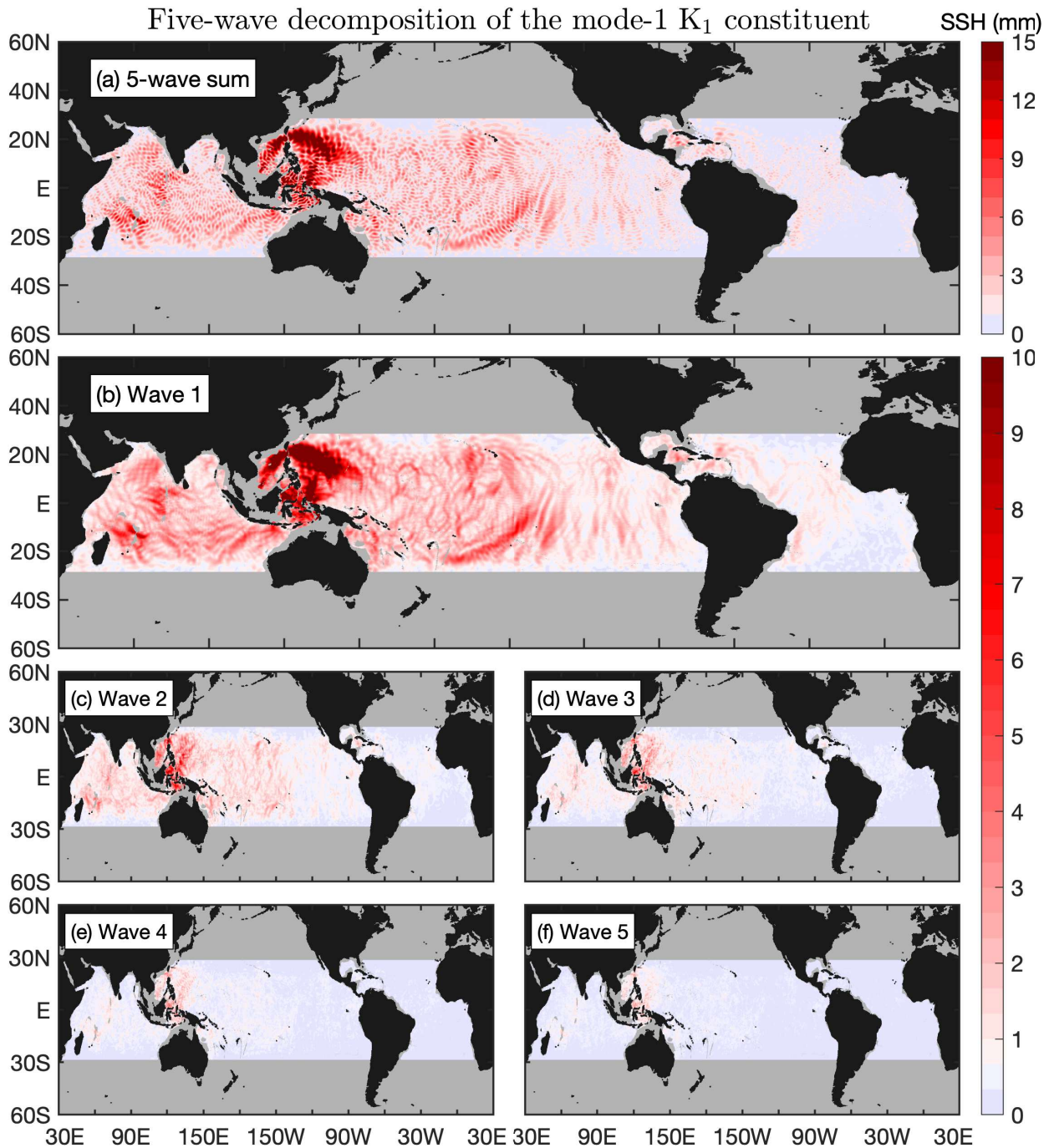


Figure S9. Five-wave decomposition of the mode-1 K_1 internal tide constituent. (a) The 5-wave sum. (b)-(f) The 5 waves. At each grid point, five mode-1 K_1 internal tidal waves in arbitrary horizontal directions are determined by plane wave analysis. Panel (b) shows well-defined long-range internal tidal beams associated with notable topographic features.

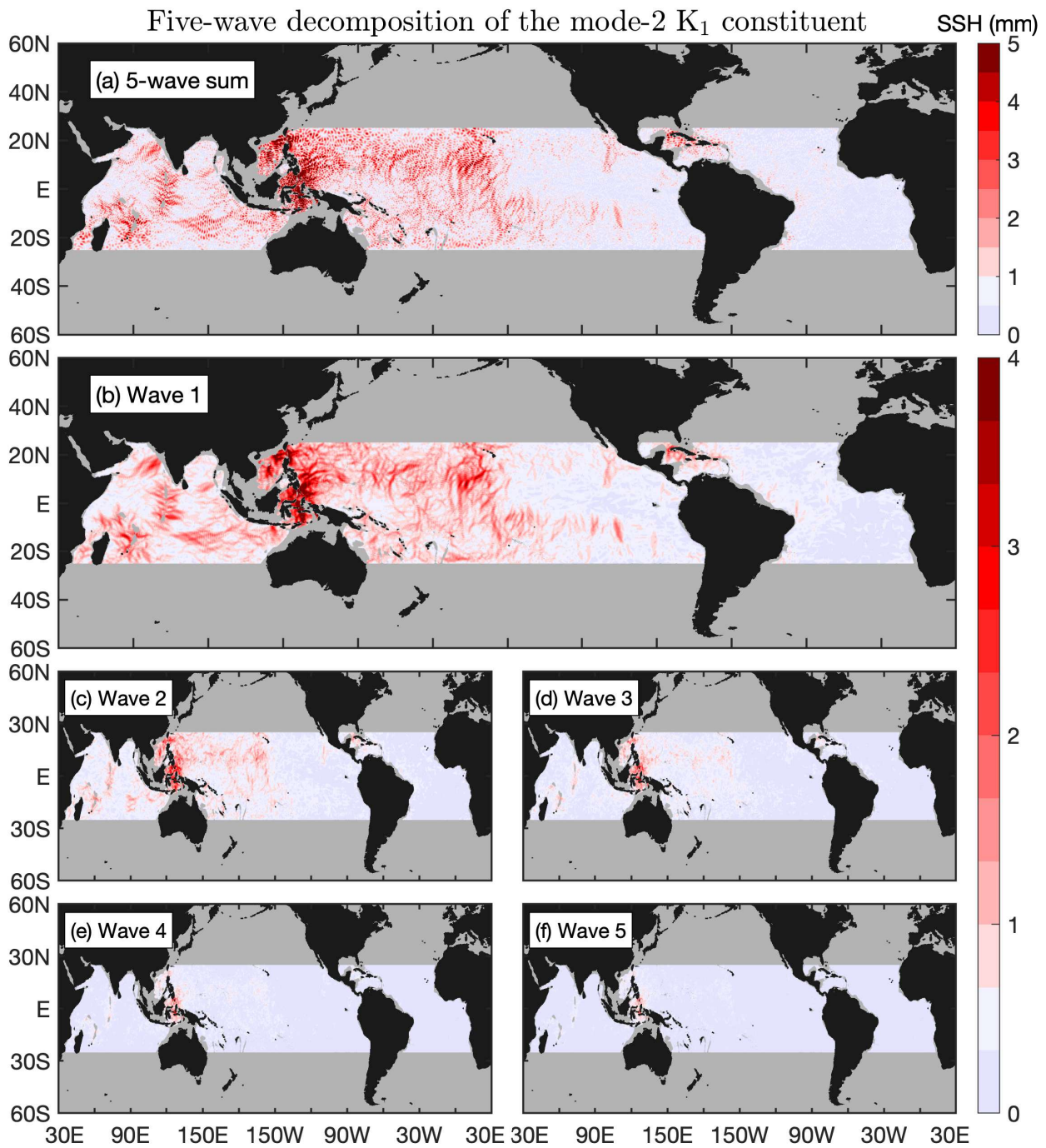


Figure S10. As in Figure S9 but for the mode-2 K_1 internal tide constituent.

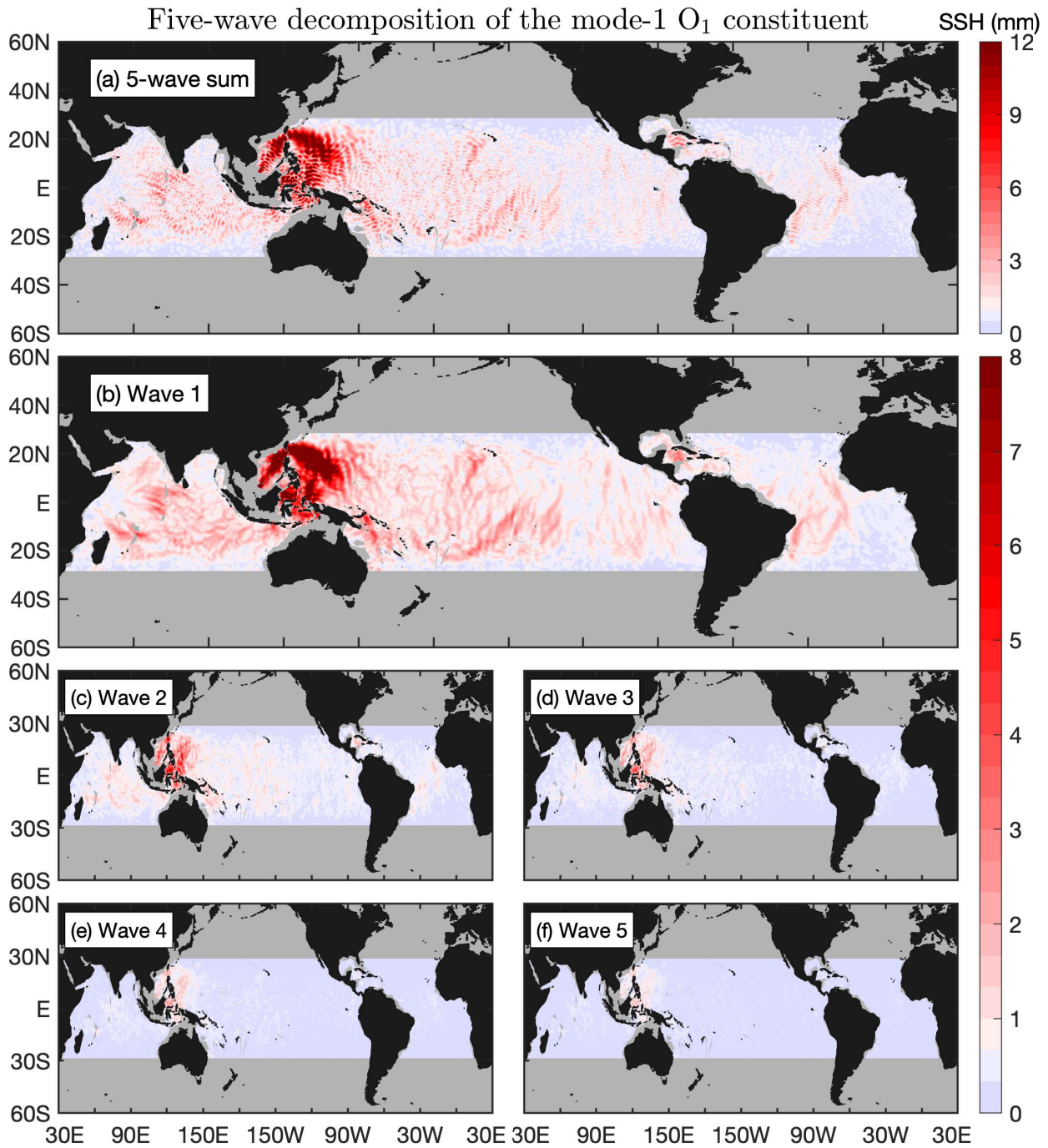


Figure S11. As in Figure S9 but for the mode-1 O_1 internal tide constituent.

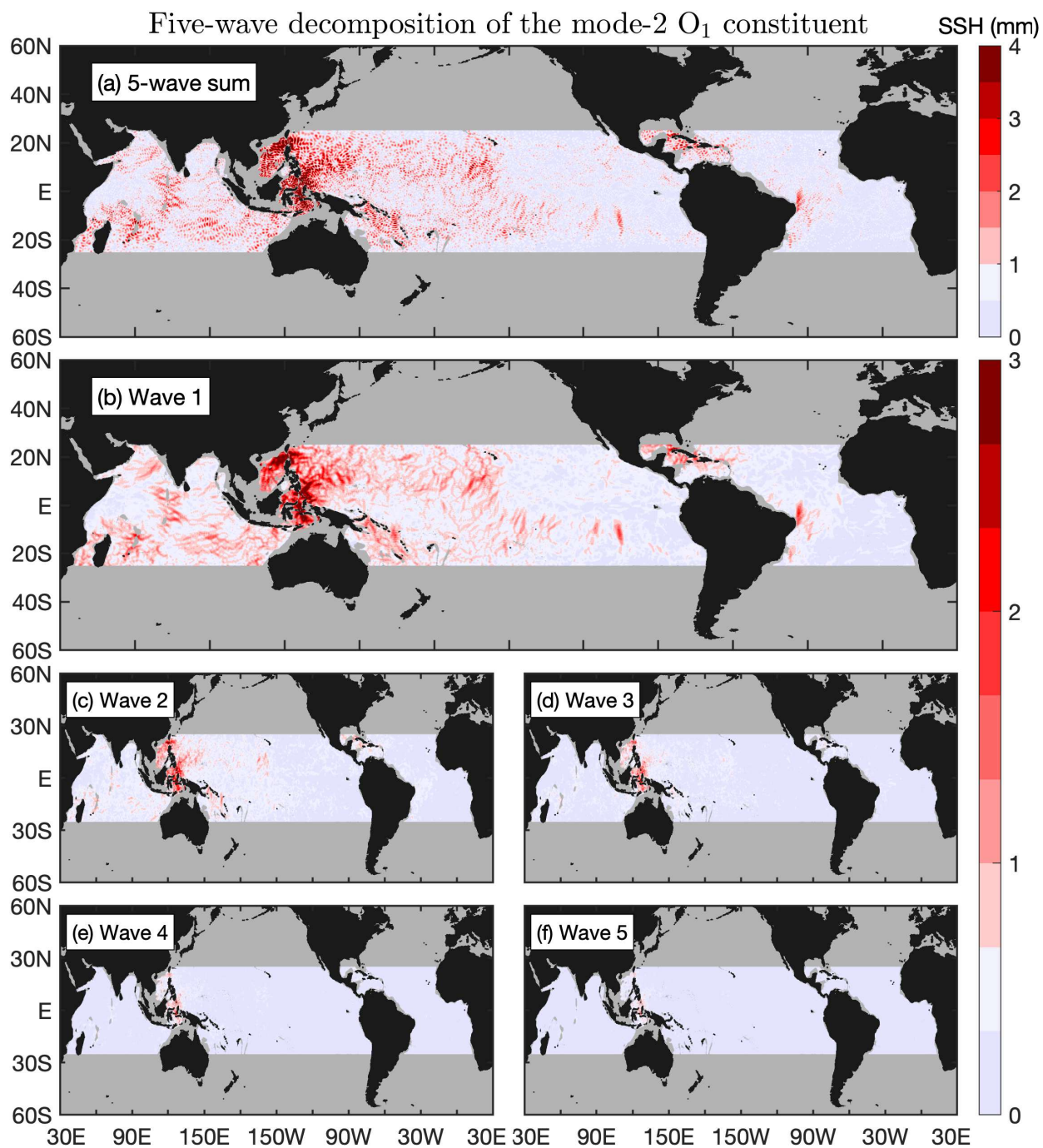


Figure S12. As in Figure S9 but for the mode-2 O_1 internal tide constituent.

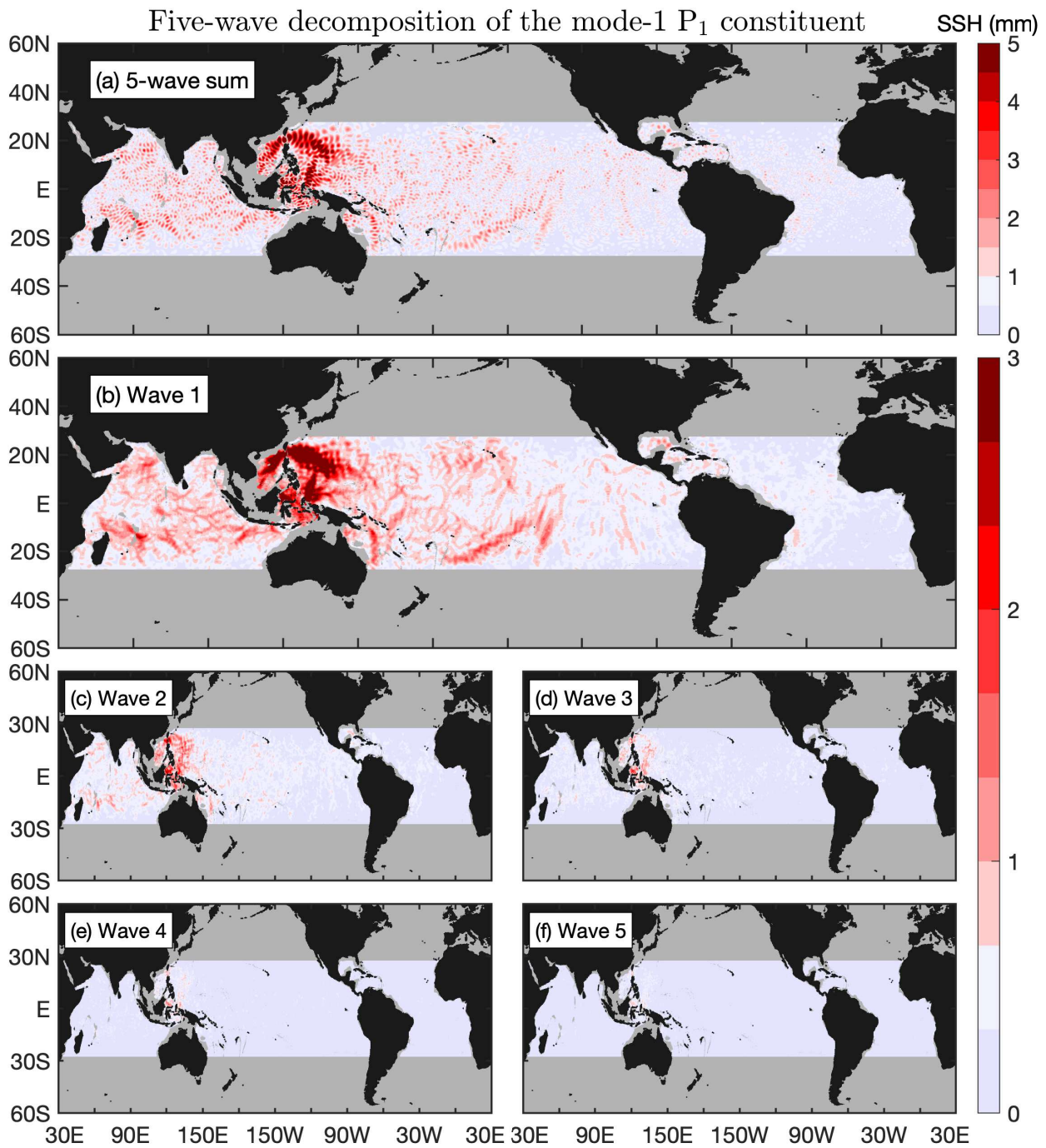


Figure S13. As in Figure S9 but for the mode-1 P_1 internal tide constituent.

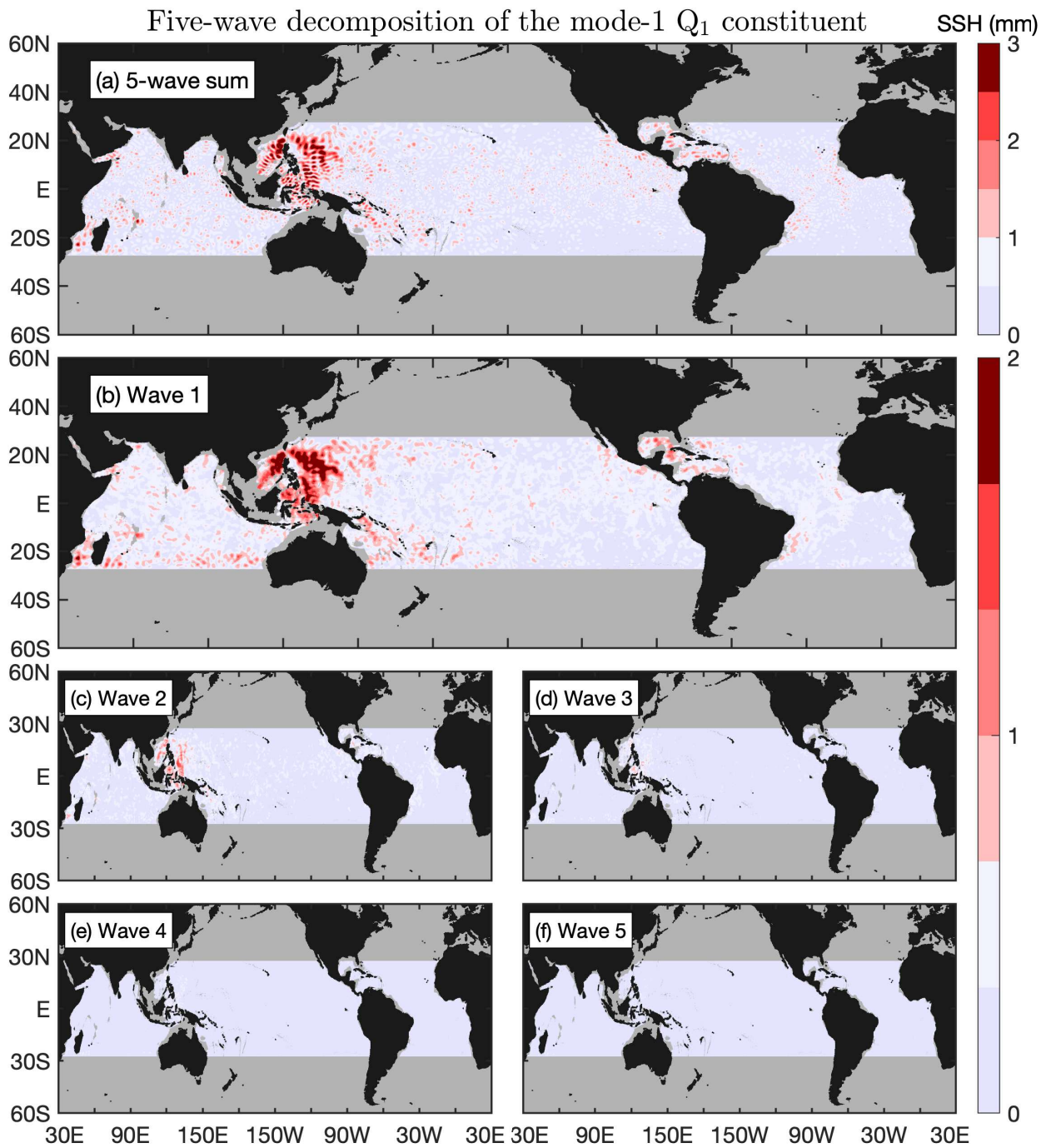


Figure S14. As in Figure S9 but for the mode-1 Q_1 internal tide constituent.

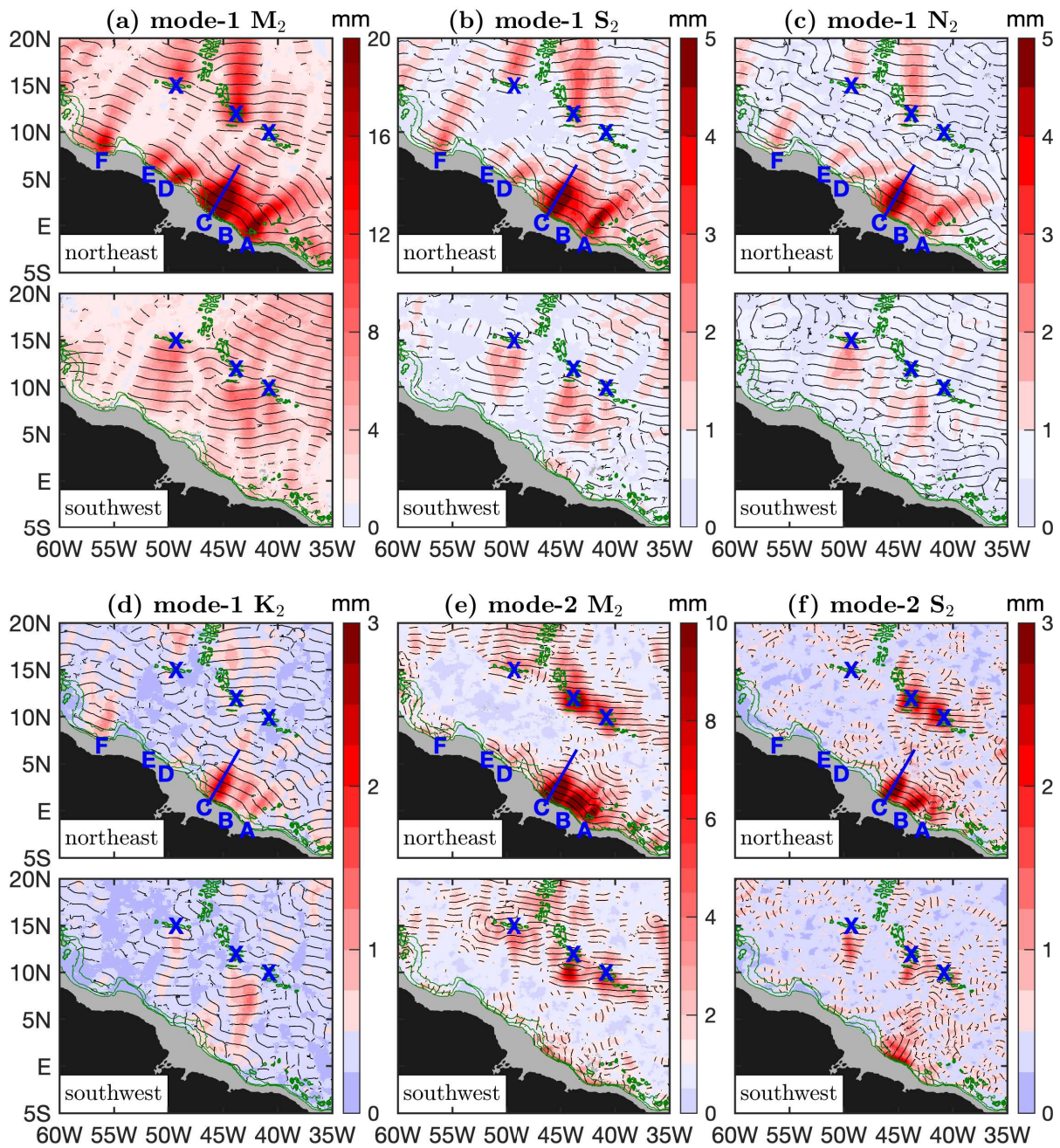


Figure S15. Semidiurnal internal tidal beams off the Amazon shelf. Each constituent is divided into northeastward (-45° – 135°) and southwestward (135° – 315°) components. Black lines indicate the 0° co-phase charts. Green contours indicate the 1000-, 2000-, and 3000-m isobaths. Isolated beams off the Amazon shelf are labeled A–F. Blue lines highlight the strongest beams generated at the mouth of the Amazon River. Beams generated at the Mid-Atlantic Ridge are marked.

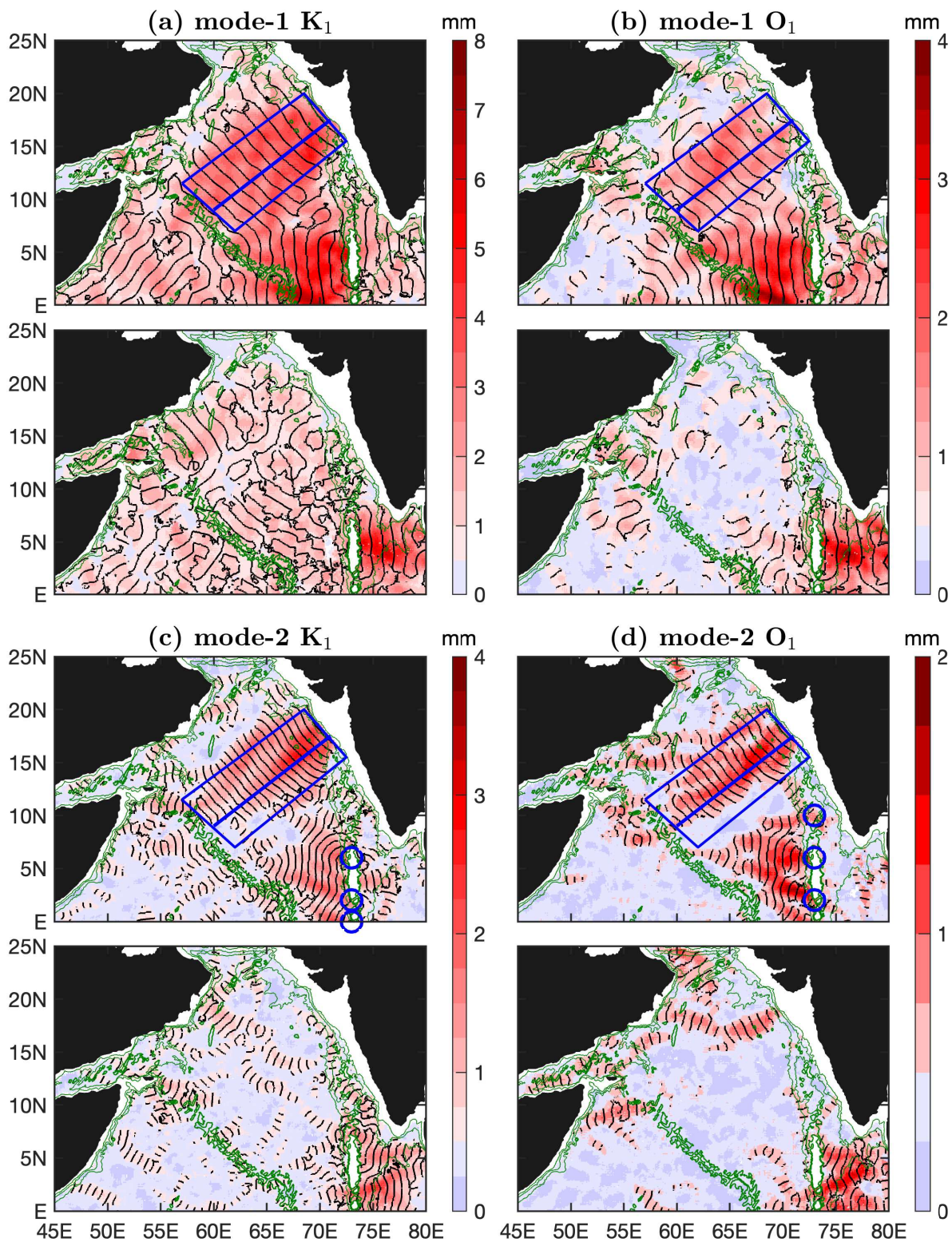


Figure S16. Diurnal internal tidal beams in the Arabian Sea. Each constituent is divided into eastward (-90° – 90°) and westward (90° – 270°) components. Internal tides with amplitudes lower than 0.5 mm are shown in light blue. Black lines indicate the 0° and 180° co-phase charts. Green contours indicate the 1000-, 2000-, and 3000-m isobaths. Blue circles mark some isolated mode-2 beams at the Chagos–Laccadive Ridge.